Renewable Energy 159 (2020) 1036–1046

Contents lists available at ScienceDirect

Renewable Energy

journal homepage: www.elsevier.com/locate/renene

Information value-based optimization of structural and environmental monitoring for offshore wind turbines support structures

Lijia Long [a, b, *], Quang Anh Mai [c], Pablo Gabriel Morato [d], John Dalsgaard Sørensen [b], Sebastian Thöns [a, e]

[a] Dept. 7: Safety of Structures, BAM Federal Institute for Materials Research and Testing, Berlin, Germany
[b] Dept. of Civil Engineering, Aalborg University, 9220, Aalborg, Denmark
[c] Renewables Certification, DNV-GL, Hamburg, Germany
[d] ANAST, Naval & Offshore Engineering, ArGEnCo, University of Liege, Liege, Belgium
[e] Department of Building and Environmental Technology, Lund University, Sweden

ARTICLE INFO

Article history:
Received 2 February 2020
Received in revised form
20 May 2020
Accepted 7 June 2020
Available online 12 June 2020

Keywords:
Structural health monitoring
Offshore wind turbine
Monopile support structure
Value of information
Weld fatigue
Decision tree
Dynamic Bayesian Network

ABSTRACT

The use of load and structural performance measurement information is vital for efficient structural integrity management and for the cost of energy production with Offshore Wind Turbines (OWTs). OWTs are dynamically sensitive structures subject to an interaction with a control unit exposed to repeated cyclic wind and wave loads causing deterioration and fatigue. This study focuses on the quantification of the value of structural and environmental information on the integrity management of OWT structures, with the focus on fatigue of welded joints. By utilizing decision analysis, structural reliability methods, measurement data, as well as the cost-benefit models, a Value of Information (VoI) analysis can be performed to quantify the most beneficial measurement strategy. The VoI assessment is demonstrated for the integrity management of a butt welded joint of a monopile support structure for a 3 MW OWT with a hub height of approximately 71m. The conditional value of three-year measured oceanographic information and one-year strain monitoring information is quantified posteriori in conjunction with an inspection and repair planning. This paper provides insights on how much benefits can be achieved through structural and environmental information, with practical relevance on reliability-based maintenance of OWT structures.

1. Introduction

Offshore wind is a rapidly growing industry and to achieve reduction of operational costs of Offshore Wind Turbines (OWTs), it is important to choose optimal maintenance strategies to be implemented on the turbine components [1]. Applications of Structural Health Monitoring (SHM) for the design and maintenance of OWT structures have gained much attention within the past few years to detect and diagnose abnormalities of windturbine components, see e.g. Ref. [2–5]. Being exposed to repeated cyclic wind and wave loads, OWTs are dynamically sensitive structures and can benefit from monitoring systems. Implementing SHM in offshore wind energy support structures can help to investigate uncertainties in design, provide input for the verification of operational conditions and possible future design optimization, predict time-dependent deterioration for maintenance planning with the aim of reducing operations and maintenance costs and possible lifetime extension to achieve longer energy generation in the future while fulfilling the requirement of reliability, functionality and sustainability [6].

An OWT includes the Rotor and Nacelle Assembly (RNA), tower, substructure and foundations which e.g. can be a jacket/tripod with piles or bukets, monopiles, mono buckets, gravity bases or moored floaters. Up to now, the most commonly used OWT foundations are monopiles [7]. For the different components of the wind turbine different SHM techniques can be applied, see Ref. [8,9]. For example

* Corresponding author. Dept. 7: Safety of Structures, BAM Federal Institute for Materials Research and Testing, Berlin, Germany.
E-mail addresses: lilo@civil.aau.dk (L. Long), anh.quang.mai@dnvgl.com (Q.A. Mai), pgmorato@uliege.be (P.G. Morato), jds@civil.aau.dk (J.D. Sørensen), sebastian.thoens@outlook.com (S. Thöns).

https://doi.org/10.1016/j.renene.2020.06.038

for monitoring the condition of the drivetrain, oil condition monitoring, acoustic emission, theomography, electromagnetical-parameter based monitoring and holistic or global condition monitoring are under research. For monitoring the rotor blades, vibration-based SHM, acoustic emissions, strain measurement and deflection based methods are under development. Sensor types for monitoring offshore support structures includes strain gauges, optical fibre sensors, temperature sensors, displacement sensors, accelerometers, inclinometers, photometers and laser interferometers. However, the techniques for blades and sub-structures are still under development, they are not industry practice yet. The operating and environmental conditions of virtually all wind turbines in operation today are recorded by the Supervisory Control And Data Acquisition (SCADA) system in 10-min intervals [8]. The minimum data set typically includes 10 min-average values of: wind speed, wind direction, active power, reactive power, ambient temperature, pitch angle and rotational speed (rotor and/or generator).

In particular the research on SHM of offshore wind energy support structures has been considerably intensified during recent years. Among the key drivers for this is the requirement in the standard from Bundesamt für Seeschifffahrt und Hydrographie (BSH) in Germany that at least 1 out of 10 OWT support structures must be equipped with a SHM system [8]. In this paper the focus is on SHM of offshore wind energy monopile support structures.

Most SHM research focuses on obtaining measurement data, extracting damage features, and deriving the damage indices e.g. miners sum of fatigue damage, without an explicit further consideration of the integrity management decision and action, see e.g. Ref. [5,10]. The scope of this paper aims to fill the gap of transforming the SHM data into knowledge that contributes to decisions of structural integrity management. Besides, among all the research related to SHM of OWTs, only few studies [11–14] focus on quantification the value of SHM in offshore wind energy support structures. The design of the SHM system is typically based on experience and limited by the budget. When improper SHM strategies are implemented, it may lead to big losses by obtaining an enormous amount of irrelevant information with high data processing costs that may trigger inappropriate remedial activities. Thus, there is a need to quantify the value of SHM in offshore wind energy support structures to improve the decision basis for implementing SHM and provide insight on how to choose the most beneficial measurement strategy. The information value-based decision analysis can be a very useful tool for the decision makers. Therefore, this paper focuses on the quantification of the conditional value of strain and wind monitoring information for maintenance of OWT monopile support structures, with emphasis on fatigue of welded joints.

To identify and quantify the most beneficial measurement strategy, a Value of Information (VoI) analysis is used, which is based on the Bayesian pre-posterior decision theory presented in Raiffa and Schlaifer (1961) [15] and Bayesian updating and utility-based decision theory to quantify the utility increase due to additional information. The expected value of SHM information can be found as the difference between the maximum utility obtained in analysis with SHM information and the maximum utility obtained without SHM information, considering the structural fatigue reliability, inspection and repair planning as well as the cost-benefit assessments. The utility increase, if additional information is already obtained at the time of decision-making, is denoted as Conditional Value of Sample Information (CSVI).

A similar proposed approach is used with great success for decision making on inspection planning for fatigue critical details in offshore structures [11,12] and the work presented in this paper is an extension to application for offshore wind energy support structures and is extended to include SHM in general. Through quantifying the value of different SHM system information, the optimal lifecycle maintenance planning can be determined, which facilitates the reliability and safety in the assets management for offshore wind energy support structures and in turn ensures a cost-efficient energy generation for sustainable societal developments.

This paper starts describing the VoI methodology and the process of quantification of the CSVI in Section 2, then Section 3 introduces a probabilistic model based on monitoring data to calculate the annual probability of failure, Section 4 describes the method of updating the annual probability failure with the inspection event, and finally Section 5 introduces a cost model and calculates the results of the conditional value of three monitoring strategies. Furthermore a parametric analysis regards the cost model is discussed in Section 6. The paper ends in Section 7 with the conclusion.

2. Value of information analysis

As described in the introduction, since the strain and wind monitoring information are already obtained at the time of decision-making, this paper focuses on the quantification of the conditional value of strain and wind monitoring information for planning the maintenance of OWT monopile support structures, with emphasis on fatigue of welded joints. Measurement of the wind speed from the SCADA system and monitoring information on stress ranges from strain gauges were obtained on a butt welded joint of the monopile support structure of a 3 MW OWT with a hub height of approximately 71m. To quantify the conditional value of the two types SHM information, a decision tree analysis is introduced.

2.1. Decision tree description

A general decision tree for Bayesian decision making contains five dimensions: information acquirement strategies $\boldsymbol{e}$, outcomes of strategies $\boldsymbol{z}$, possible actions $\boldsymbol{a}$, system states $\boldsymbol{\theta}$ and its consequences. An illustration of the decision tree process is shown in Fig. 1 with three branches: The base decision scenario is without monitoring e_0, one scenario with only wind monitoring information e_1 and one scenario with both wind and strain monitoring information e_2. With different monitoring strategies, the optimal planing of the total inspection times N_I and year t_{N_I} will be different. The outcome $\boldsymbol{z}$ describes the inspection outcome, e.g. detection of a crack (D) or no detection of a crack ($\overline{D}$), which is denoted with a chance node (circle). The action $\boldsymbol{a}$ contains the possible actions, like Do nothing (N) or Repair (R), which is represented with a rectangle. The system state $\boldsymbol{\theta}$ can be Failure (F) or Safe (S). The consequence of failure of a welded joint is assumed to be unscheduled repair, which is shown as a diamond. A decision rule is introduced, which is shown by a dashed decision node (rectangle). The dashed rectangle indicates inspections and repairs that will be repeated during the service life. In this paper, the decision rules are: if no detection of a crack, the action will be doing nothing, otherwise repair is done immediately after detection of a crack. The welded joints can only be repaired after inspection. The welded joints need to be inspected if the annual probability of failure reaches a certain threshold.

2.2. Conditional value of sample information calculation

The CSVI can be calculated by subtracting the expected total costs of the base decision scenario e_0 from the expected total costs from the enhanced decision scenario with obtained wind

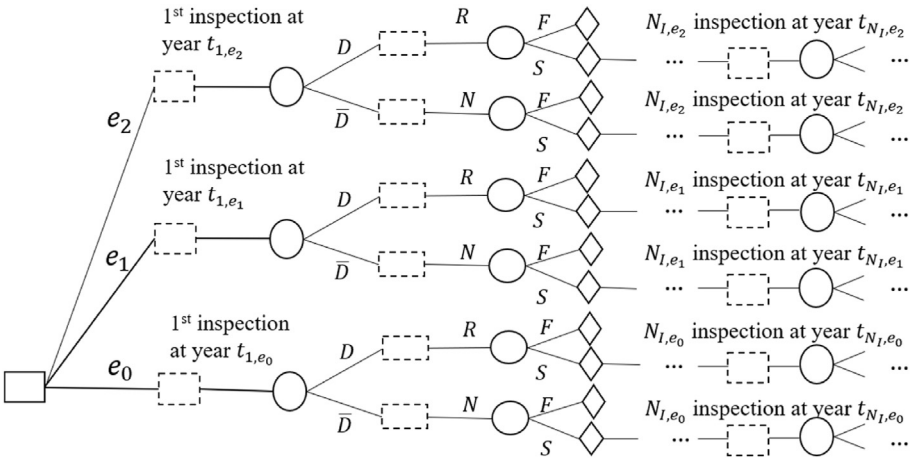

Fig. 1. Decision tree of comparing beneficial measurement strategy regards to improve future inspection and repair planning.

monitoring e_1 or both wind and strain information e_2:

$$CVSI(e_i) = E[C_T(e_0), T_{SL}] - E[C_T(e_i), T_{SL}] \tag{1}$$

For each monitoring strategy e_i, the decision tree will repeat its branch for every inspection outcome. Assuming that in total that there will be N_j branches (N_j types of combination of continous inspection outcomes) until the end of service life T_{SL}, each branch has its probability of occurrence, $P(j)$. The expected total life cycle costs $E[C_T(e_i), T_{SL}]$ of strategy e_i are the sum of all branches of expected inspection costs $E[C_I(e_i,j), T_{SL}]$, expected repair costs $E[C_R(e_i, j), T_{SL}]$, expected failure costs $E[C_F(e_i,j), T_{SL}]$ during service life and the monitoring costs C_M when monitoring is applied.

$$E[C_T(e_i),T_{SL}]=\sum_{j=1}^{N_j} P(j)\cdot(E[C_I(e_i,j),T_{SL}]+E[C_R(e_i,j),T_{SL}]+E[C_F(e_i,j),T_{SL}] \times)+C_M(e_i) \tag{2}$$

$P(j)$ is the product of probabilities of continous inspection outcomes during life cycle, e.g. the product of probability of detecting a crack P_D at each inspection year if damage is detected everytime after inspection during the service life. For each branch the expected costs of inspection, repair and failure can be calculated as follows [16,17]:

$$E[C_I(e_i,j), T_{SL}] = \sum_{n=1}^{N_{I,e_i,j}} C_I \cdot \left(1 - P_F\left(t_{N_{I,e_i,j}}\right)\right)\cdot \frac{1}{(1+r)^{t_{N_{I,e_i,j}}}} \tag{3}$$

$$E[C_R(e_i,j), T_{SL}] = \sum_{n=1}^{N_{R,e_i,j}} C_R \cdot P_R\left(t_{N_{R,e_i,j}}\right) \cdot \left(1 - P_F\left(t_{N_{R,e_i,j}}\right) \times\right) \cdot \frac{1}{(1+r))^{t_{N_{R,e_i,j}}}} \tag{4}$$

$$E[C_F(e_i,j), T_{SL}] = \sum_{t=1}^{T_{SL}} \Delta P_{F,e_i,j}(t) \cdot C_F \cdot \frac{1}{(1+r))^t} \tag{5}$$

r is the discounting rate. T_{SL} is service life. $N_{I,e_i,j}$ is the total number of inspections with monitoring strategy e_i in branch j. $N_{R,e_i,j}$ is the total number of repairs with monitoring strategy e_i in branch j. $t_{N_{I,e_i,j}}$ is the inspection year at N_I inspection time with strategy e_i in branch j. $P_F(t_{N_{I,e_i,j}})$ is the accumulated probability of failure at inspection year $t_{N_{I,e_i,j}}$. $t_{N_{R,e_i,j}}$ is the repair year at N_R, denoting the repair time with strategy e_i in branch j. $P_R(t_{N_{R,e_i,j}})$ is the probability of repair at repair year $t_{N_{R,e_i,j}}$ which will be equal to $P_D(t_{N_{R,e_i,j}})$ as the repair action will be taken immediately when the damage is detected. $P_F(t_{N_{R,e_i,j}})$ is the accumulated probability of failure at repair year $t_{N_{R,e_i,j}}$. $\Delta P_{F,e_i,j}$ is the anaual probability of failure with monitoring strategy e_i in branch j. C_I is the inspection cost per time, C_R is the repair cost per time, C_F is the failure cost, which describes the unscheduled repair cost in this paper.

In the following, Section 3 will first introduce how to calculate P_F and ΔP_F based on probabilistic fatigue models integrated with monitoring data, then Section 4 will present how to predict inspection year t_{N_I}, the inspection times N_I, how to simulate P_D and update the ΔP_F from Section 3 based on inspection outcomes. Finally Section 5 will introduce the cost model of C_I, C_R, C_F, r and present the CSVI results.

3. Probabilistic fatigue model

In this paper, the failure probability of the support structure is first updated considering the SHM data in a stress-life (S–N) approach and then considering the crack inspection data in a fracture mechanics (FM) approach. The FM model is calibrated from the posterior S–N model.

There are two types of monitoring information considered in the calculation, representing two levels of SHM investment:

- Only the meteo-oceanographic data, i.e. wind speed, wave height, wave period, etc.
- Both the meteo-oceanographic data and the strain data, where the duration of concurrent measurement of the two types of data is long enough to consider most of the important load combinations, e.g. one year duration.

It is assumed that the SHM campaign is started from the beginning of the service life. At the time of assessment, three years of wind monitoring data and one year of strain data is available. The strain data measured at the same time with the wind data is used to relate wind speed distribution to the fatigue damage in the limit state function. If only the meteo-oceanogaphic data is available, the stress data can be obtained from finite element analyses.

In this section, the methodology to consider SHM data is summarized, a more detailed explanation can be found in Ref. [18].

3.1. Bayesian updating of the wind speed distribution

The wind measurement data is used to update the long-term wind speed distribution which in turn, is used in the limit state function to calculate the updated failure probability. The prior distribution of the long-term wind speed distribution is established using the design wind speed distribution and 15-year data of the 10-min mean wind speed before construction.

The long-term wind speed distribution is assumed to follow a Weibull distribution of which the scale parameter k_w is considered normally distributed with unknown mean μ and unknown standard deviation σ, see Eq. (6).

$$f_{K_w}(k_w|\mu,\sigma)=f_N(k_w|\mu,\sigma)=\frac{1}{\sigma\sqrt{2\pi}}\exp\left(-\frac{1}{2}\left(\frac{k_w-\mu}{\sigma}\right)^2\right) \tag{6}$$

The new information is the estimated values of k_w, obtained by fitting the measured 10-min mean wind speed data of each year into a Weibull distribution of which the shape parameter is the same as the design value.

The predictive density function of k_w given measured data becomes a Student's t-distribution as shown in Eq. (7).

$$f_{K_w}\left(k_w|\widehat{\mathbf{k}}_w\right)=f_s\left(k_w|\mu'',s''\frac{n''+1}{n''},\nu''\right)$$
$$=\frac{\Gamma\left(\frac{\nu''+1}{2}\right)}{s''\sqrt{\nu''\pi}\Gamma\left(\frac{\nu''}{2}\right)}\left[\frac{\nu''+\left(\frac{k_w-\mu''}{s''}\right)^2}{\nu''}\right]^{-\frac{\nu''+1}{2}} \tag{7}$$

where:

- μ'', s'', n'', ν'' are the posterior parameters and μ', s', n', ν' are the prior parameters of the expectation of mean $(E[\mu])$, the expectation of the standard deviation $(E[\sigma])$, the sample size (n), and degrees of freedom (ν), respectively.
- the prior parameters are asymptotically given as:
  - $E[\mu]=\mu'$
  - $E[\sigma]=s'$
  - $V[\mu]=\frac{s'}{\mu'\sqrt{n'}}$
  - $V[\sigma]=\frac{1}{2\nu'}$
- The prior parameters of the Student' t-distribution of k_w are established using the design wind speed distribution and the 15-year wind measurement data before construction:
  - $\mu'=k_w^{design}=10.4$ (m/s)
  - $n'=15$, $\nu'=15-1=14$
  - to calculate s', it is assumed that the coefficient of variation of the mean value $(V[\mu])$ equals to that of the annual mean wind speeds of the 15-year data: $V[\mu]=0.042$, so that $s'=V[\mu]\cdot\mu'\sqrt{n'}=1.68$
- the posterior parameters are calculated as following, using n years of measurement data:
  - $n''=n'+n$
  - $\mu''=\frac{n'\mu'+n\overline{k}_w}{n''}$
  - $s''^2=\frac{\nu's'^2+n'\mu'^2+\nu s^2+n\overline{k}_w^2-n''\mu''^2}{\nu''}$
  - $\nu''=\nu'+\delta(n')+\nu+\delta(n)-\delta(n'')$
- the statistical $\overline{k}_w$ and s^2 quantities are calculated for the vector of the $\widehat{\mathbf{k}}_w$ - a vector of n components corresponding to n years of wind measurement $\widehat{\mathbf{k}}_w=(\widehat{k}_{w,1},\ \widehat{k}_{w,2},\ \cdots,\ \widehat{k}_{w,n})$ as following:
  - $\overline{k}_w=\frac{1}{n}\sum_{i=1}^{n}\widehat{k}_{w,i}$
  - $s^2=\frac{1}{n-1}$
  - $\nu=n-1$

Equation (7) is the probability density function of the random variable k_w in the limit state functions Eq. (8) and Eq. (11).

3.2. Probabilistic model for strategy $\boldsymbol{e}_0$

Before updating the long-term distribution of wind speed using measurement data, the failure probability of a welded joint can be calculated taking into account the predictive density function of k_w in Eq. (7). In this case, the posterior parameters (i.e. μ'', s'', n'', and ν'') are equal to the prior parameters.

The limit state function is based on the Palmgren-Miner rule:

$$g=\Delta-D_{total} \tag{8}$$

where Δ is the critical fatigue damage and D_{total} is total fatigue damage summed up from each bin of wind speed and from each year in the service life. The citical fatigue damage is the threshold to justify when fatigue fracture happens. A lognormal distribution with median equal 1.0 and CoV equals to 0.3 as proposed by Wirsching [29] can be used to represent Δ. Given that the stress-ranges obtained from measurement data correspond to the lower branch of the bi-linear S–N curve, the limit state function in Eq. (8) can be developed as:

$$g=\Delta-\sum_{i=1}^{T}\sum_{j=1}^{n_{U_{10}}}\frac{\left(\alpha_f X_m X_{SCF}\right)^{m_2}}{K}k_{s,j}^{m_2}\Gamma\left(\frac{m_2}{\lambda_{s,j}}+1\right)P(U_{10,j}|k_{w,i})\frac{n_{c,j}}{n_{m,j}}n_m^* \tag{9}$$

where:

T the service life in years.
$n_{U_{10}}$ number of bins of wind speed.
α_f the strain extrapolating factor from the measuring location to the location of interest.
K the random variable represents the uncertainty in the S–N curve, without having tested data established for specific design and fabrication, a typical standard deviation $\sigma_{\log K}=0.2$ is suggested by DNV-RP-C203 [19]. The mean value is calculated from the charactristic value of the chosen S–N curve.
m_2 the negative slope of the lower branch of the S–N curve.
X_m the random variable represents the uncertainty in strain measurement, When there is no experimental data available for a specific site, Thöns [13] suggested to use a normal distribution with mean of 1 and standard deviation of 0.05.
X_{SCF} the random variable represents the uncertainty in the stress concentration factor, This uncertainty depends on the complexity of the joint and the method to calculate stress concentration factor. In this paper, a lognormal distribution with mean of 1 and standard deviation of 0.15 is used, following the background document to IEC 61400.1 ed 4 [20].
$U_{10,j}$ the 10-min mean wind speed in the j^{th} bin.
$k_{w,i}$ the random variable represents the scale parameter of the Weibull long-term wind speed distribution at the i^{th} year.
$k_{s,j}$ the scale parameter of the Weibull stress-range distribution of the j^{th} bin of wind speed.
$\lambda_{s,j}$ the shape parameter of the Weibull stress-range distribution of the j^{th} bin of wind speed.
$n_{c,j}$ number of stress cycles in the j^{th} bin of wind speed.
$n_{m,j}$ number of wind speed records in the j^{th} bin of wind speed.
n_m^* total observed wind speed records per year.

Given the lower and upper bounds of the j^{th} bin of wind speed are a_j and b_j, $P(U_{10,j}|k_{w,i})$ can be estimated as in Eq. (10), where F_W is the cumulative probability function of the Weibull distribution and λ_w is the design shape parameter.

$$P(U_{10,j}|k_{w,i}) = F_W(a_j \le U_{10} < b_j; k_{w,i}, \lambda_w) = \exp\left(-\left(\frac{a_j}{k_{w,i}}\right)^{\lambda_w}\right) - \exp\left(-\left(\frac{b_j}{k_{w,i}}\right)^{\lambda_w}\right) \quad (10)$$

The uncertainties used in Eq. (9) are detailed in Table 1:

3.3. Probabilistic model for strategy $\boldsymbol{e}_1$ and $\boldsymbol{e}_2$

Given T_m years of wind measurement, the fatigue damage of the measurement years are known to be related to the fatigue loading. The corresponding scale parameters $k_{w,i}$ in Eq. (9) should be treated as deterministic, i.e. using directly the fitted values. The limit state function in Eq. (9) can be rewritten as Eq. (11):

$$g = \Delta - \sum_{i=1}^{T_m}\left(D_i\middle|\widehat{k}_{w,i}\right) - \sum_{j=T_m+1}^{T}\left(D_j|k_{w,j}\right) \quad (11)$$

where.

$\widehat{k}_{w,i}$ is the i^{th} component of the vector $\widehat{\mathbf{k}}_w$,
$k_{w,j}$ is the predicted value of k_w at the year j^{th},
D_i is fatigue damage of year i^{th}, $i = 1\cdots T_m$, defined in Eq. (12):

$$D_i = \sum_{j=1}^{n_{U_{10}}} \frac{(\alpha_f X_m X_{SCF})^{m_2}}{K} k_{s,j}^{m_2}\Gamma\left(\frac{m_2}{\lambda_{s,j}}+1\right)P(U_{10,j}|\widehat{k}_{w,i})\frac{n_{c,j}}{n_{m,j}}n_m^* \quad (12)$$

D_j is the fatigue damage of year j^{th}, $j = T_m + 1\cdots T$, defined similar to D_i but use $k_{w,j}$ instead of $\widehat{k}_{w,i}$.

3.4. Annual probability of failure

The failure probability limit state function in Eqs. (9) and (11) can be solved using a first order reliability method (FORM) as well as simulation techniques, see e.g. Ref. [21]. The updated failure probability after considering SHM is used to calibrate the FM model inSection 4. Afterward, the updated failure probability of the FM model is used with the cost model inSection 5. The annual failure probability calculated hereafter is to be used in the cost model. The annual failure probability of year t given survival up to year $(t-1)$ is calculated as:

$$\Delta P_F(t) = \frac{P_F(t) - P_F(t-1)}{1 - P_F(t-1)} \quad (13)$$

For the comparison of the VoI in this paper, failure probabilities are calculated and updated for three scenarios:

- When wind and strain monitoring data is available (e_2): the stress-range distribution is fitted for each bin of wind speed to get $\lambda_{s,j}$ and the mean of $k_{s,j}$,
- When only wind monitoring data is available (e_1): the scale parameters $k_{s,j}$ of the fitted stress-range distributions are scaled to yield the design fatigue damage (in this case, it is assumed that the joint is design to the limit).
- Without monitoring data (e_0): the design wind speed distribution is used together with the stress-range distributions in e_1.

Instead of modifying the fitted stress-range distributions in e_0 for e_1 and e_2, it is possible to use the stress-range histograms available from the design data (or perform finite element analyses using the measured wind data) to fit the distribution for each bin of wind speed.

The annual failure probabilities of the three cases are shown in Fig. 2. It can be seen that using only three years of wind data, the annual failure probability is not reduced as significantly as the case where both wind and strain data is available. It means the measured wind conditions are foreseen in the design wind speed distribution and the design stress-range distribution is conservative.

4. Updating the reliability based on inspections/repairs

In this section, the reliability of the welded joints is updated based on the information gathered from inspections. First, a fracture mechanics model is presented to quantify the deterioration and is calibrated to match the reliability estimated in Section 3. Then, an inspection model is introduced to quantify the measurement quality. The reliability is updated thereafter based on the inspection outcomes.

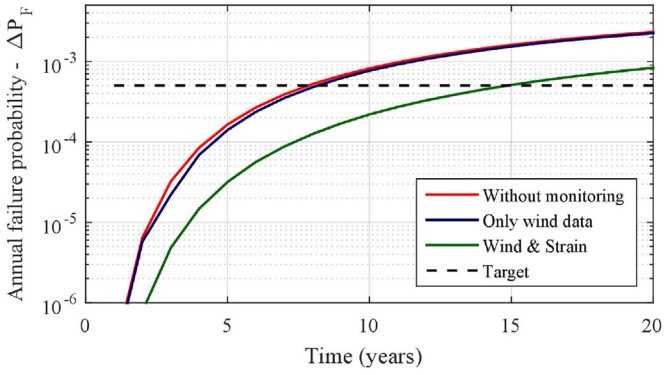

Fig. 2. Annual probability of failure.

Table 1
Details of input random variables.

RVs	Distribution	Mean or Median	CoV or Std.	Comment
Δ	Lognormal	$\bar{m} = 1$	CoV = 0.3	following DNV-GL [19]
X_m	Normal	$\mu = 1$	CoV = 0.05	following Thöns [13]
X_{SCF}	Lognormal	$\mu = 1$	CoV = 0.15	following Sørensen [20]
K	Lognormal	$\mu_{\log K} = 16.006$	$\sigma_{\log K} = 0.2$	following DNV-GL [19]
$k_{s,j}$	Normal	fitted	CoV = 0.1	assumed; fitted $\lambda_{s,j}$ is deterministic
$k_{w,i}$	Student's t	updated	updated	$\lambda_{w,i} = \lambda_{w,design}$

Table 2
Fracture mechanics model parameters.

Variable	Distribution	Mean	CoV
a_0	Exponential	*Calibrated	–
m	Deterministic	3	–
lnC	Normal	*Calibrated	*Calibrated
S	Deterministic	19.46	–
Y	Deterministic	0.24 (Assumed)	–
n	Deterministic	$2.41 \cdot 10^7$	–

4.1. Fatigue deterioration - Fracture mechanics model

The deterioration of the structural component is estimated with the use of a SN curve/Miner's rule model during the design stage. Nevertheless, it is not possible to measure damage directly on the structure. Thus, a fracture mechanics model - which is calibrated to match the reliability obtained with the SN curve model - is preferred so as to quantify in-service deterioration. This way, the reliability can be updated once a crack has (or has not) been detected.

The linear elastic fracture mechanics (LEFM) model used in this paper is based on the Paris' law and has been derived from the formula proposed by Ref. [22]. The crack depth as function of the stress cycles can be computed according to Eq. (14).

$$a(n) = \left[\left(1 - \frac{m}{2}\right) C \pi^{m/2} S^m Y^m n + a_0^{1-m/2}\right]^{(1-m/2)^{-1}} \tag{14}$$

where, $a(n)$ stands for the crack depth and is growing as function of the number of cycles (n). C and m represent the crack growth parameters and depend on the material. The loading is incorporated through the equivalent stress range S of the measured stress-ranges from section 3 and the geometric correction factor Y which can be assumed to be a constant for simplification. The fatigue load uncertainty X_m as mentioned in Table 1 is already considered in the SN model, so it is implicitly included in the calibrated FM model. Thus, once the initial crack size a_0 is known, the crack growth over time can be computed.

A limit state is formulated in Eq. (15) to estimate the reliability of the welded joints. The failure criterion is assumed here as through-thickness crack; thus, the critical crack size a_c is defined as the plate thickness. If the number of cycles per year is assumed constant, the reliability can be computed for each year t.

$$g_{FM}(t) = a(t) - a_c \tag{15}$$

The values assigned to the fracture mechanics model are listed in the Table 2. Note that some parameters are calibrated to match the SN model's reliability.

4.1.1. Calibration of the fracture mechanics model

The initial crack size a_0 and the crack growth parameter C are calibrated to match the SN curve/Miner's reliability. A least squares optimization is conducted with the objective function Eq. (16) to minimize the error between Miner's and fracture mechanics reliability.

$$\{\mu_{a_0}, \mu_{lnC}, \sigma_{lnC}\} = \underset{\mu_{a_0}, \mu_{lnC}, \sigma_{lnC}}{argmin} \sum_{t=1}^{t_{SL}} \left(\beta_{SN}(t) - \beta_{FM}(t, \mu_{a_0}, \mu_{lnC}, \sigma_{lnC}) \right)^2 \tag{16}$$

The annual reliabilities from the calibration are illustrated in Fig. 3 and the calibrated parameters are listed in Table 3. It can be seen that while μ_{a_0} and σ_{lnC} remain similar, μ_{lnC} varies for each case.

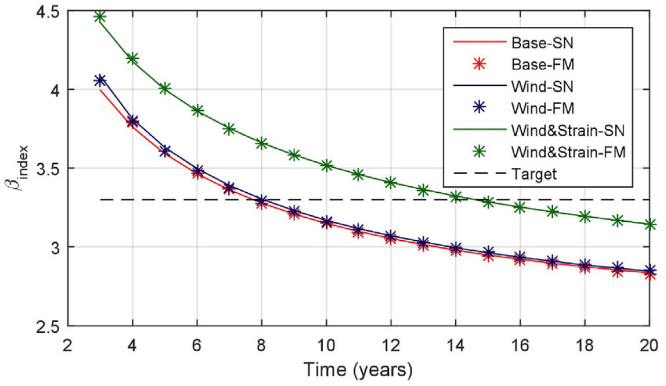

Fig. 3. Calibration of the fracture mechanics model. The line in red colour represents the base case e_0, blue colour stands for the case where the reliability is updated considering wind data e_1, and green colour for the case when both wind and strain e_2 are used for the updating. The dashed line corresponds to the target reliability. (For interpretation of the references to colour in this figure legend, the reader is referred to the Web version of this article.)

Table 3
Calibrated parameters of the fracture mechanics model.

Parameter	Base case ($\boldsymbol{e}_0$)	Wind only ($\boldsymbol{e}_1$)	Wind and strain ($\boldsymbol{e}_2$)
μ_{a_0}	$8.54 \cdot 10^{-2}$	$8.54 \cdot 10^{-2}$	$8.54 \cdot 10^{-2}$
μ_{lnC}	− 26.3	− 26.4	− 26.8
σ_{lnC}	0.9	0.9	0.9

Since the reliability increased after the update considering both strain and wind data, the resulting crack growth (μ_{lnC}) is smaller, leading to a higher reliability than the other to cases. A similar reasoning can be reached for the case when the update is only carried out considering wind data, but in this instance, the crack growth is slightly smaller than the base case.

4.2. Inspection quality - Probability of detection

During the operational life of the structure, knowledge can be gained through inspections, updating the reliability of the structural component accordingly. Yet, inspections have uncertainty associated as the measurement instrument is not perfect as well as other environmental (or human) factors that can influence the final outcome. This measurement uncertainty is commonly documented by the Probability of Detection (PoD) curves. The PoDs represent the ability of detection of a specific inspection method as function of the defect size.

Eddy current inspection is an applicable inspection method for an OWT welded joint. Since, it is not required to remove the coating before the inspection, it presents an advantage with respect to magnetic particle inspection methods. In this paper, it is assumed that eddy current inspections will be conducted and the corresponding PoD curve is documented in the DNV-GL Standard RP-210 [23], as expressed in Eq. (17). Where a is again the crack depth and the distribution parameters are defined as $X_0 = 0.45$mm and $b = 0.9$.

$$PoD(a) = 1 - \frac{1}{1 + \left(\frac{a}{X_0}\right)^b} \tag{17}$$

4.3. Updating the reliability - Dynamic Bayesian Network

The reliability of the structural component is herein computed and updated by means of a Dynamic Bayesian Network (DBN). A DBN is a type of Bayesian network where the random variables and their dependencies are represented through subsequent time steps. DBNs are also denoted as Two-Timeslice Bayesian Networks (2TBN) state-space because only the initial state and the transition space are sufficient to define the whole model. The interested reader is directed to Ref. [24,25] for a more detailed description and treatment of DBNs.

The reliability could also be computed and updated by means of Monte Carlo simulations, where a limit state is formulated for the detection event to compute the failure probability conditional on the detection outcome, as proposed by Ref. [22]. However, DBNs have increasingly gained popularity due to their computational benefits and robustness for Bayesian updating, as demonstrated by Refs. [26].

The DBN employed herein is illustrated in Fig. 4. The chance node a corresponds to the crack depth and it is dependent on the crack growth node C. In case an inspection is performed, a node Z is added and stands for the probability of detection, which is dependent on the crack size distribution. Finally, the binary node E assigns the failure probability depending on the last state of the node a. The subscripts of the nodes indicate the temporal evolution of the random variables: a_0 and C stand for the initial crack depth and crack growth parameter respectively, then, the random variables evolve from year 1 ($t = 1$) until the end of the lifetime ($t = T$).

4.3.1. Dynamic Bayesian network - Inference

In this investigation, inspections are planned based on the decision rule of conduction an inspection the year before the target reliability is reached. The target reliability defined by the Standard IEC 61400–1:2019 [27] is selected as reference, with reliability values of $\beta = 3.3$ ($\Delta P_F = 5 \cdot 10^{-4}$ with a one year reference period). Besides, it is considered that a repair will be performed once a crack is detected. After the repair, it is assumed that the welded joints will behave as a new joints following [30–32].

The reliability of the welded joints can be updated by including evidence in the DBN. More specifically, evidence gathered through inspections is included in the inspection nodes Z (Fig. 4). Once the evidence is added, the probability distribution of the subsequent nodes conditional on the inspection outcome can be inferred through a prediction inference routine. Herein, the forward operation proposed by Ref. [26] is employed for the prediction task.

4.3.2. Inspection updating - Results

The reliability of the welded joints is computed and updated according to the decision tree presented in Fig. 1 and by means of the DBN introduced in Fig. 4. The annual failure probability for all the different cases is displayed in Figs. 5–7. The inspections are represented in the figures by pointers, if the outcome is 'not-detected', the pointer is a circle and if the outcome is 'detected', the pointer is an asterisk. The annual failure probability threshold is plotted with a red line.

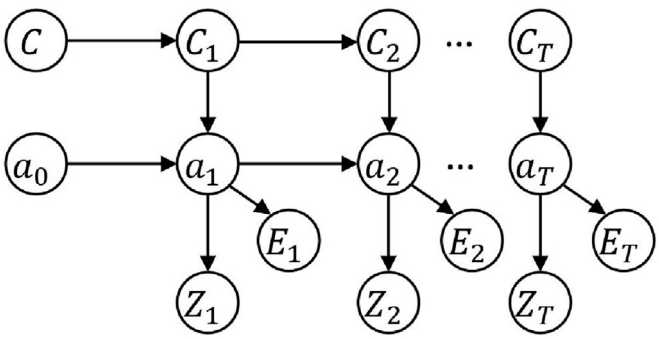

Fig. 4. Inspection updating - DBN representation.

5. Quantification the conditional value of SHM information

Based on the results from Section 4, the prediction of the number of inspections and inspection years will be different whether with or without monitoring information. The summary is shown in Table 4. t_{N_I} is the inspection year of N_I inspection times, z_{N_I} is the outcome of the N_Ith inspection time. The service life of the OWT is assumed to be 20 years. Without monitoring (e_0), the welded joints of the monopile need to be inspected three times or two times depending on the outcome of previous inspection as well as whether the planned inspection year is within the service life or not. With strategy e_1, the predicted inspections times of the welded joints will be the same namely three times or two times. But the inspections can be done slightly later with e_1 compared to e_0. However in strategy e_2, when incorporating both wind and strain monitoring data, the welded joints are only required to be inspected one time during service life.

An example of a sequential decision tree which is describing the inspection and repair plan of the base case e_0 is shown in Fig. 8. There are in total seven branches in the decision tree. The first inspection is at year 7. If a crack is detected after inspection at year 7 and repaired, the second inspection will be at year 14. If no crack is detected at year 7, the second inspection will be at year 11. Based on the outcome of the second inspection, the third inspection could be at year 18 or 16. Similar to the sequential decision tree of the base case e_0, the decision tree of the case with only wind monitoring data e_1 will have five branches, with the first inspection at year 8, second inspection at year 16 when a crack is detected and repaired at year 8 or at year 12 if no crack is detected at year 8. If no crack is detected at year 12, then the welded joints need a third inspection at year 16. With both wind and strain monitoring e_2, the welded joints only need to be inspected one time at year 14. That's because the predicted annual failure probabilities from e_2 information are much smaller than those with e_1 and e_0 information, which leads to a longer operation period before reaching the target probability for the first inspection after commissioning of the structure.

Following the formula of quantification of the VoI in Section 2 and the costs model shown in Table 5 from Ref. [28], with the results of annual probability of failure in Section 3 and the results of the probability of detection in Section 4, the value of the three monitoring strategies are quantified. When the inspection cost C_I is €1 10^4, repair cost C_R is €8 10^4, failure costs C_F (unexpected repair costs) is €1.5 10^5, cost of wind monitoring C_w is €5 10^2 which only accounts for the data processing fee due to the SCADA system already being installed in the commissioning stage, cost of strain monitoring C_s is €1 10^3 and discounting rate r is 0.02, the CVSI of wind (e_1) is €1.7 10^4 and the CVSI of wind and strain (e_2) is €4.2 10^4.

By spending 0.9% of total service life costs of strategy e_0 to obtain first three-year wind monitoring information of e_1, up to 30% of lifecycle management costs of e_0 can be saved. Even though there is a slight difference of inspection years between e_0 and e_1 (slightly later inspection years in e_1), with e_1 there will be a higher chance of only inspecting two times during the service life while with e_0 it is more likely that there will be three inspections, which leads to a positive CSVI of e_1. By spending 2.6% of total costs of e_0 to acquire the wind monitoring data of the first three-year period and one-year strain monitoring information in e_2, up to 73% of life cycle

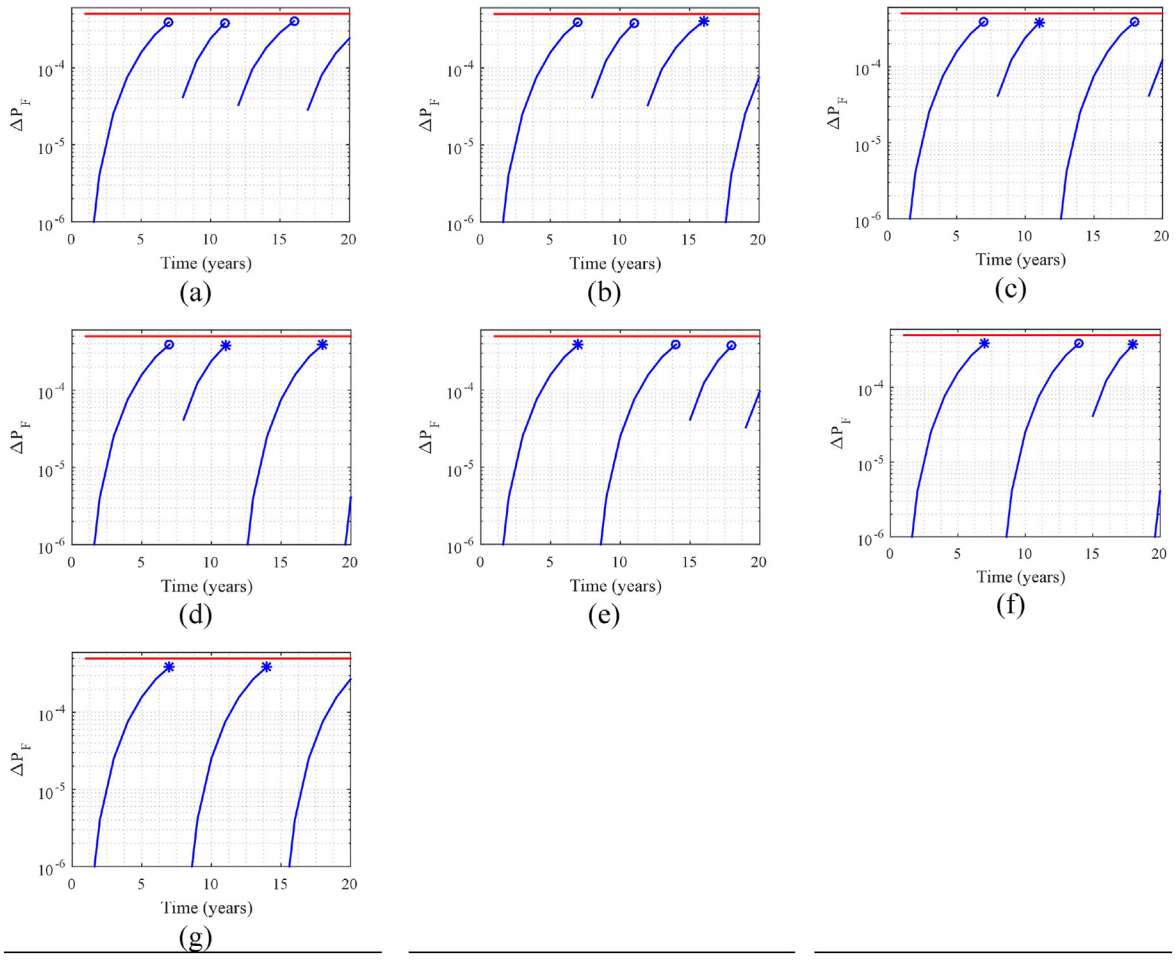

Fig. 5. Inspection updating - Base case.e_0

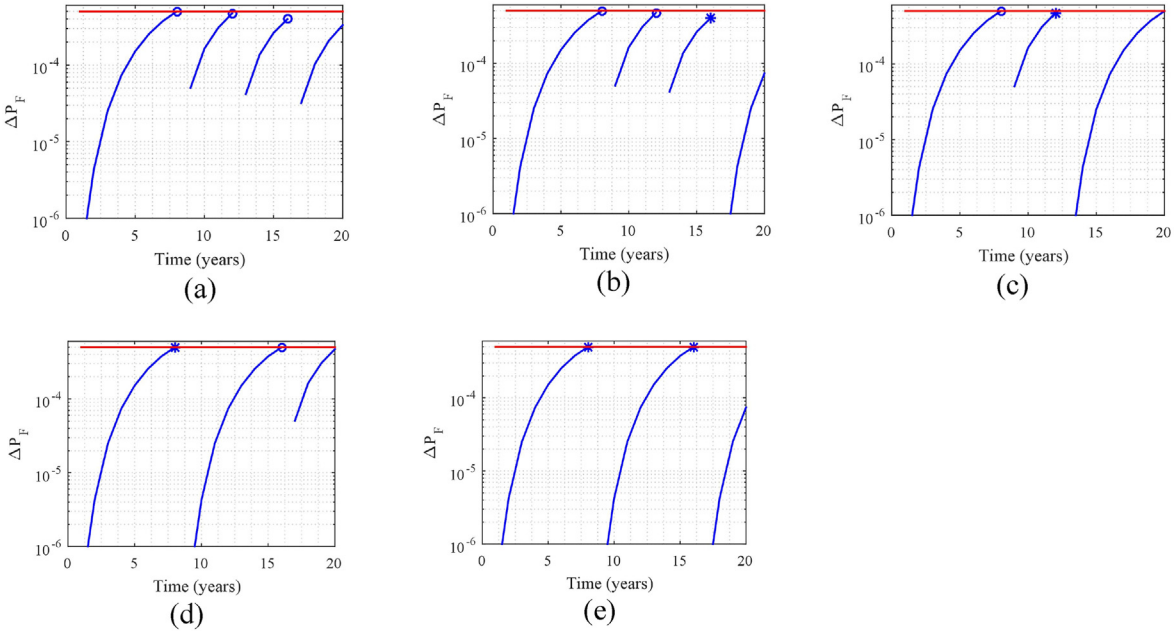

Fig. 6. Inspection updating - Only wind case.e_1

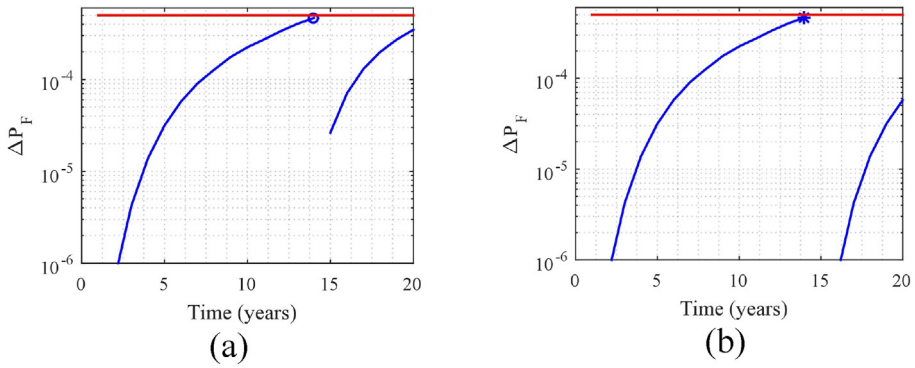

Fig. 7. Inspection updating - Wind & strain case.e_2

Table 4
Summary of the inspection plan for the three cases.

Base case ($\boldsymbol{e}_0$)					Wind only ($\boldsymbol{e}_1$)					Wind & strain ($\boldsymbol{e}_2$)	
$N_I = 1$		$N_I = 2$		$N_I = 3$	$N_I = 1$		$N_I = 2$		$N_I = 3$	$N_I = 1$	
t_{N_I}	z_{N_I}	t_{N_I}	z_{N_I}	t_{N_I}	t_{N_I}	z_{N_I}	t_{N_I}	z_{N_I}	t_{N_I}	t_{N_I}	z_{N_I}
7	D_7	14	D_7, D_{14}	23	8	D_8	16	D_8, D_{16}	26	14	D_{14}
	$\overline{D}_7$	11	$D_7, \overline{D}_{14}$	18		$\overline{D}_8$	12	$D_8, \overline{D}_{16}$	21		$\overline{D}_{14}$
			$\overline{D}_7, D_{11}$	18				$\overline{D}_8, D_{12}$	20		
			$\overline{D}_7, \overline{D}_{11}$	16				$\overline{D}_8, \overline{D}_{12}$	16		

management costs of e_0 can be saved, due to the significantly reduction of inspection times. Thus the combination of the strain and wind monitoring strategy e_2 is more beneficial than only the wind monitoring strategy e_1, and even more beneficial than without monitoring e_0 for this case.

Table 5
Summary of costs model.

C_I	C_R	C_F	C_w	C_s	r
€1 10^4	€8 10^4	€1.5 10^5	€5 10^2	€1 10^3	0.02

6. Parametric analysis

With respect to cost of failure C_F, inspection cost C_I, repair cost C_R and discounting rate r, the parametric analysis on CVSI is investigated. The results are shown in Fig. 9. With the increase of cost of failure C_F, the CVSI of e_2 and e_1 keep almost constant (a) and the CVSI of e_2 will always be higher than the CVSI of e_1, showing that the cost of failure will not influence the choice of CVSI. This is because of the applied "target threshold" decision rule, which will make the cost of failure not influence the number of inspection times and year. With increase of the cost of inspection C_I (b) and cost of repair C_R (c), the CVSI is increasing. However the difference between e_2 and e_1 is becoming larger with the increase of the cost of inspection C_I. The CVSI is decreasing with the increase of the discounting rate r as shown in (d). The CVSI of e_2 is higher than the

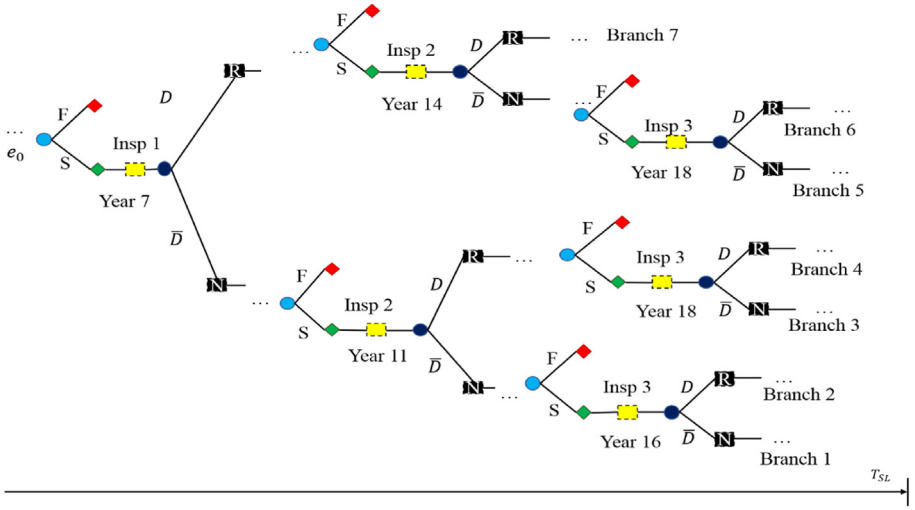

Fig. 8. Sequential decision tree of base case.e_0.

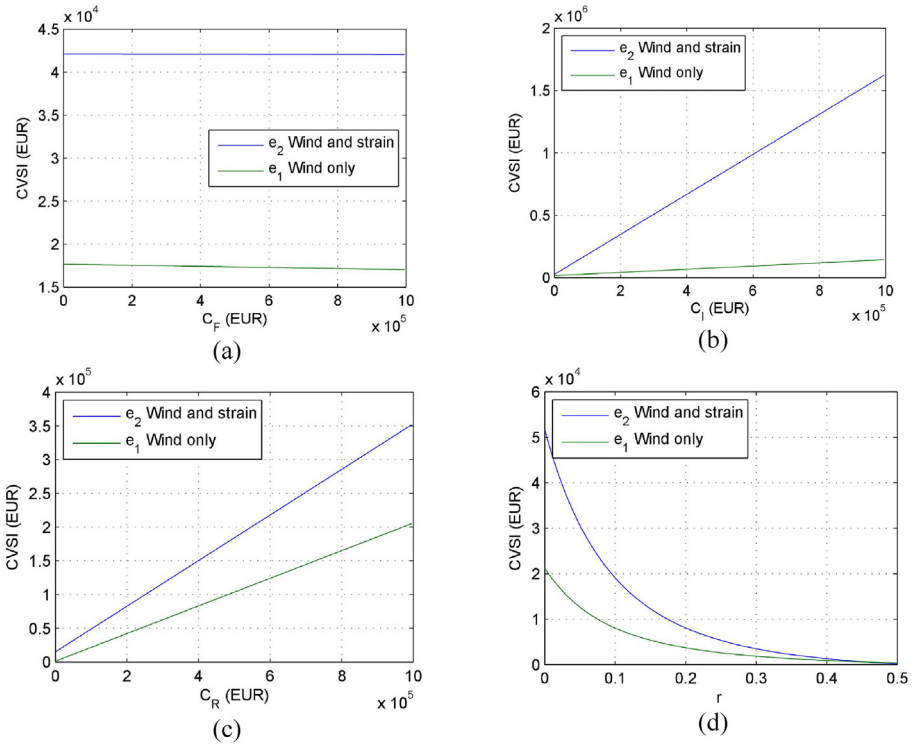

Fig. 9. CSVI independence of C_F, C_R, C_I.r

CVSI of e_1 when the discounting rate is less than 0.4. The difference between the CVSI of e_1 and e_2 is becoming smaller with increasing disconting rate. When the discounting rate is larger than 0.4, both CVSI of e_1 and e_2 become around zero, which is because the money becomes less valuable with higher discounting rate, so that it will not add value to invest on monitoring at all.

From Fig. 9 (a)–(d), it can be seen that the CVSI of e_2 is alomost always higher than the CVSI of e_1 with changes of C_F, C_R, C_I and r, which shows that the cost models will not change the fact that the combination of the strain and wind monitoring strategy e_2 is more beneficial than only the wind monitoring strategy e_1. It is however dependent on the measurement outcome. In our case the one-year strain monitoring has shown smaller fatigue loads than what can be seen from three-year wind measurements. The fatigue loads shown from the three-year wind measurements appear slightly smaller than what is expected from design. In this case the expected number of inspection and repair times from e_2 will be smaller than e_1 and the CVSI of e_2 will be higher than e_1.

7. Conclusions

Early research proposed different SHM techniques for the OWT, recent studies have improved on that by suggesting methods to quantify the value of SHM information. This work highlights that the optimal monitoring strategy for offshore wind energy support structures can be deterimined posteriori through conditional value of structural and environmental information analysis. The application on the quantification of the conditional value of three-year measured oceanographic information and one-year strain monitoring information on a butt welded joint of a monopile support structure of OWT shows that the combination of the strain and wind monitoring strategy is more beneficial than only the wind monitoring strategy, which is again better than without monitoring. However, this is based on the fact that the monitoring results have shown smaller fatigue loads than expected from design. Therefore for future research, the understanding of scenarios when the monitoring shows contrary results, e.g. strain monitoring indicates larger fatigue loads than what can be seen from the wind monitoring, will be critically important if aiming to do pre-posterior decision analysis before implementaion of SHM. This presented research work provides a decision basis for lifecycle structural integrity management by quantifying the value of structural and environmental information, with the ultimate goal to contribute to cost-efficient and sustainable energy generation through maintaining the reliability and serviceability of offshore wind energy support structures.

Funding

This research work was performed within the European project INFRASTAR (infrastar.eu), which has received funding from the European Union's Horizon 2020 research and innovation program under the Marie Skłodowska-Curie grant agreement No 676139. The grant is gratefully acknowledged.

CRediT authorship contribution statement

Lijia Long: Writing - original draft, Writing - review & editing, Investigation, Methodology, Software, Formal analysis. **Quang Anh Mai:** Data curation, Methodology, Software, Writing - review & editing. **Pablo Gabriel Morato:** Validation, Methodology, Software, Writing - review & editing. **John Dalsgaard Sørensen:** Supervision, Conceptualization. **Sebastian Thöns:** Supervision.

Declaration of competing interest

The authors declare that they have no known competing financial interests or personal relationships that could have

appeared to influence the work reported in this paper.

Acknowledgements

The support of COST Action TU1402 on Quantifying the Value of Structural Health Monitoring is gratefully acknowledged. The authors would like to thank the reviewers for the insightful and constructive review.

References

[1] H. Seyr, M. Muskulus, Decision support models for operations and maintenance for offshore wind farms: a review, Appl. Sci. 9 (2019) 278.
[2] W. Yang, R. Court, J. Jiang, Wind turbine condition monitoring by the approach of SCADA data analysis, Renew. Energy 53 (2013) 365–376.
[3] A. Kusiak, W. Li, The prediction and diagnosis of wind turbine faults, Renew. Energy 36 (2011) 16–23.
[4] E. Lapira, D. Brisset, H.D. Ardakani, D. Siegel, J. Lee, Wind turbine performance assessment using multi-regime modeling approach, Renew. Energy 45 (2012) 86–95.
[5] A.A. Khan, S. Zafar, N. Khan, Z. Mehmood, History current status and challenges to structural health monitoring system aviation field, J. Spacecraft Technol. 4 (2014) 67–74.
[6] A. Rahim, P. Sparrevik, A. Mirdamadi, Structural Health Monitoring for Offshore Wind Turbine Towers and Foundations, Offshore Technology Conference, Offshore Technology Conference, 2018.
[7] W. Europe, The European Offshore Wind Industry—Key Trends and Statistics 2016, Wind Europe, Brussels, Belgium, 2017, p. 37.
[8] K. Fischer, D. Coronado, Condition Monitoring of Wind Turbines: State of the Art, User Experience and Recommendations, Fraunhofer-IWES, Bremerhaven, 2015.
[9] R. Rolfes, S. Tsiapoki, M. Häckell, Sensing Solutions for Assessing and Monitoring Wind Turbines, Sensor technologies for civil infrastructures, Elsevier, 2014, pp. 565–604.
[10] C.R. Farrar, K. Worden, Structural Health Monitoring: a Machine Learning Perspective, John Wiley & Sons, 2012.
[11] S. Thöns, M.H. Faber, D.V. Val, On the value of structural health monitoring information for the operation of wind parks, in: Proceedings of the Safety, Reliability, Risk, Resilience and Sustainability of Structures and Infrastructure, 12th International Conference on Structural Safety and Reliability, Wien Vienna, Austria, 2017, pp. 6–10.
[12] S. Thöns, Monitoring based condition assessment of offshore wind turbine support structures, IBK Bericht (2012) 345.
[13] S. Thöns, R. Schneider, M.H. Faber, Quantification of the Value of Structural Health Monitoring Information for Fatigue Deteriorating Structural Systems, 12th International Conference on Applications of Statistics and Probability in Civil Engineering, 2015.
[14] A. May, D. McMillan, S. Thöns, Economic analysis of condition monitoring systems for offshore wind turbine sub-systems, IET Renew. Power Gener. 9 (2015) 900–907.
[15] H. Raiffa, R. Schlaifer, Applied Statistical Decision Theory, Division of Research, GraduateSchool of Business Administration, Harvard University, Boston, 1961. RaiffaApplied Statistical Decision Theory1961, DOI.
[16] A. Agusta, S. Thöns, On the development of tools for decision analyses, in: 1st International Conference on Structural Integrity for Offshore Energy Industry, 2018.
[17] D. Straub, Generic approaches to risk based inspection planning for steel structures, Vdf Hochschulverlag 284 (2004). AG.
[18] Q.A. Mai, W. Weijtjens, C. Devriendt, P.G. Morato, P. Rigo, J.D. Sørensen, Prediction of remaining fatigue life of welded joints in wind turbine support structures considering strain measurement and a joint distribution of oceanographic data, Mar. Struct. 66 (2019) 307–322.
[19] G. Dnv, Fatigue Design of Offshore Steel Structures, Recommended Practice DNVGL-RP-C203, 2016, p. 20.
[20] J.D. Sørensen, Reliability-based Calibration of Fatigue Safety Factors for Offshore Wind Turbines, the Twenty-First International Offshore and Polar Engineering Conference, International Society of Offshore and Polar Engineers, 2011.
[21] H.O. Madsen, S. Krenk, N.C. Lind, Methods of Structural Safety, Courier Corporation, 2006.
[22] O. Ditlevsen, H.O. Madsen, Structural Reliability Methods, Wiley, New York, 1996.
[23] G. Dnv, Dnv Gl, in: Probabilistic Methods for Planning of Inspection for Fatigue Cracks in Offshore Structures, Standard No. DNVGL-RP-C210, Oslo, Norway, 2015.
[24] K.P. Murphy, S. Russell, Dynamic Bayesian Networks: Representation, Inference and Learning, 2002.
[25] D. Koller, N. Friedman, Probabilistic Graphical Models: Principles and Techniques, MIT press, 2009.
[26] D. Straub, Stochastic modeling of deterioration processes through dynamic Bayesian networks, J. Eng. Mech. 135 (2009) 1089–1099.
[27] J. Sørensen, H. Toft, Safety Factors–IEC 61400-4-background Document, DTU Wind Energy-E-Report-0066 (EN), 2014.
[28] M. Martinez-Luengo, M. Shafiee, Guidelines and cost-benefit analysis of the structural health monitoring implementation in offshore wind turbine support structures, Energies 12 (2019) 1176.
[29] P.H. Wirsching, Fatigue reliability for offshore structures, J. Struct. Eng. 10 (1984) 2340–2356.
[30] D. Straub, Generic Approaches to Risk Based Inspection Planning for Steel Structures, PhD. thesis, Chair of Risk and Safety, Institute of Structural Engineering. ETH Zürich., 2004.
[31] M.H. Faber, J.D. Sørensen, J. Tychsen, D. Straub, Field implementation of RBI for jacket structures, J. Offshore Mech. Arctic Eng. 127 (3) (2005) 220–226.
[32] A. Agusta, S. Thöns, On the development of tools for decision analyses, in: 1st International Conference on Structural Integrity for Offshore Energy Industry, Aberdeen , United Kingdom, September 6 - 7, 2018.